

Local laser heating effects in diamond probed by photoluminescence of SiV⁻ centers at low temperatures

Cite as: Appl. Phys. Lett. **124**, 091101 (2024); doi: [10.1063/5.0184331](https://doi.org/10.1063/5.0184331)

Submitted: 25 October 2023 · Accepted: 5 February 2024 ·

Published Online: 26 February 2024





View Online



Export Citation



CrossMark

Yuanfei Gao,^{1,2}  Jia-Min Lai,¹  Zhen-Yao Li,¹  Ping-Heng Tan,¹  Chong-Xin Shan,^{3,a)}  and Jun Zhang^{1,a)} 

AFFILIATIONS

¹State Key Laboratory of Superlattices and Microstructures, Institute of Semiconductors, and Center of Materials Science and Optoelectronics Engineering, University of Chinese Academy of Sciences, Chinese Academy of Sciences, Beijing 100083, People's Republic of China

²Beijing Academy of Quantum Information Sciences, Beijing 100193, People's Republic of China

³Henan Key Laboratory of Diamond Optoelectronic Materials and Devices, Key Laboratory of Material Physics, Ministry of Education, School of Physics and Microelectronics, Zhengzhou University, Zhengzhou 450052, People's Republic of China

^{a)}Authors to whom correspondence should be addressed: cxshan@zzu.edu.cn and zhangjwill@semi.ac.cn

ABSTRACT

The accurate measurement of thermal conductivity of diamond below 10 K has always been a challenge, mainly due to significant error in temperature sensing using the thermocouple method. Diamond is generally considered to have high thermal conductivity, so little attention has been paid to the laser heating effects. Here, we observed the dynamic redshift and broadening of zero phonon line of silicon-vacancy (SiV⁻) centers at 4 K. Utilizing the intrinsic temperature response of the fine structure spectra of SiV⁻ as a probe, we confirmed that laser heating effect appears and the temperature rising results from high defect concentration. By simulating the thermal diffusion process, we have estimated the thermal conductivity of around 1 W/(m K), which is a two-order magnitude lower than that of single-crystal diamond. Our results provide a feasible scheme for all-optical non-contact temperature sensing and help to solve the problem of accurate measurement of thermal conductivity at cryogenic temperatures.

Published under an exclusive license by AIP Publishing. <https://doi.org/10.1063/5.0184331>

Diamond is considered to possess high thermal conductivity due to low mass of carbon atoms, strong interatomic bonding in lattice, and low anharmonicity of the interatomic potential.¹ It is a promising material used for heat dissipation of high-power semiconductor devices, which are key to delivering high-efficiency energy conversion in power electronics systems.² It is well known that heating due to decreased thermal conductivity will degrade the performance of semiconductor devices.² Thermal conductivity strongly depends on impurity concentration. Nitrogen could present in a large concentration, which reduces the thermal conductivity by several times.³ In addition, diamond shows a strong isotope effect: diamond grown with the isotopically enriched C¹² could increase the value of thermal conductivity up to 50% at room temperature.^{4,5} Thus, the large uncertainty of thermal conductivity hinders the application of diamonds in optoelectronic devices, especially in extreme environments. Recently, thermal conductivity of three synthetic single-crystal diamonds was measured with high accuracy at temperatures from 6 to 410 K.⁶ The thermal

conductivity was measured by a steady-state longitudinal heat flow method. However, this method is not suitable for thermal conductivity measurement locally below 10 K, mainly due to the inaccuracy of temperature difference measurement. Therefore, it is important to find an alternative temperature measurement method for estimating thermal conductivity at low temperatures.

Nanoscale sensing based on atom-like solid-state systems is promising in metrology.⁷⁻¹¹ Diamond has lots of advantages in local temperature sensing. It is chemically and physically inert and has low toxicity, which is considered to have a minimal effect on the cell functionality.¹² There are many color centers with excellent optical properties in diamond, such as nitrogen-vacancy (NV) center^{13,14} and silicon-vacancy (SiV) center.^{15,16} The color centers have attracted particular interest for their robustness to extreme environments and for their ability to be localized within nanometers. The electron spin of NV centers could be used to probe magnetic, temperature, electric, and strain fields within nanometers and high sensitivity.^{7-9,17,18}

However, it has a limitation since it requires the application of microwave radiation. Microwave radiation cannot be focused below a small size and can produce heating effects. A possible alternative to the NV center may be silicon-vacancy (SiV^-) center or the recently discovered germanium vacancy (GeV^-) center,^{19–22} which has optical spectra dominated by a zero-phonon line (ZPL), offering a possibility to measure temperature by the optical method. At low temperatures, the SiV^- center's ZPL has been observed to split into a four-line fine structure, which is regarded as a “spectral fingerprint” of the SiV^- center in a high-quality, low-stress diamond. The fluorescence of SiV^- centers is predominantly concentrated in the purely electronic transition, and the ZPL features a room temperature width of down to 0.7 nm^{23} due to weak electron-phonon coupling interaction. Extremely narrow line-width provides a high sensitivity for temperature measurement, which is not available with other fluorescent probes. Thus, we can measure the temperature evolution using micro-PL spectra of SiV^- center as a probe at low temperature.

Here, by measuring the fine structure spectra of SiV^- centers at low temperatures, we observe PL spectra of the upper and lower surfaces of bulk diamond exhibit different dependencies on the excitation power. Under high-power excitation, the spectra show obvious redshift and broadening. By calibrating with the intrinsic temperature dependence of the SiV^- spectra, we confirm that the evolution of the spectra resulted from laser heating effects in the center of the laser spot. Through theoretical analysis, the temperature rising in the center of

the spot is determined by the relatively low thermal conductivity. By measuring the defect concentration distribution, we confirmed the large doping of defects and the lattice imperfection in the initial growth greatly reduced the thermal conductivity. By simulating the thermal diffusion process, we estimate the thermal conductivity of diamond has reduced by nearly two orders of magnitude than that of high-quality single-crystal diamond. It is shown that the fine structure spectrum of SiV^- centers could be a sensitive probe for laser heating effects in diamonds. In addition, it is an alternative way to estimate the thermal conductivity of diamonds at low temperatures.

Figures 1(a) and 1(b) show the basic characterization of the MPCVD diamond. The XRD shows only one peak located at about 119.9° , which proves that the diamond is mono-crystalline. The (400) peak consists of two sub-peaks, which come from the $\text{Cu } K\alpha_1$ and $\text{Cu } K\alpha_2$ line; the splitting of the XRD peak suggests high crystal quality.²⁴ The inset shows the optical image in which the sample is nearly colorless and transparent. The absorption spectrum is shown in Fig. S2. There is a sharp absorption edge at around 5.5 eV , which corresponds to the bandgap of diamond in Fig. 1(b) that shows the Raman spectra of the CVD diamond located at 1332 cm^{-1} with a full width at half maximum (FWHM) of 2.3 cm^{-1} at the lower surface and 2.2 cm^{-1} at the upper surface, respectively. Therefore, it suggests that the sample grown by MPCVD has a high crystalline quality. In homoepitaxial CVD diamond films with high crystalline quality, the ZPL of the SiV^- centers splits into four fine structure peaks at 4 K. Figures 1(c) and 1(e)

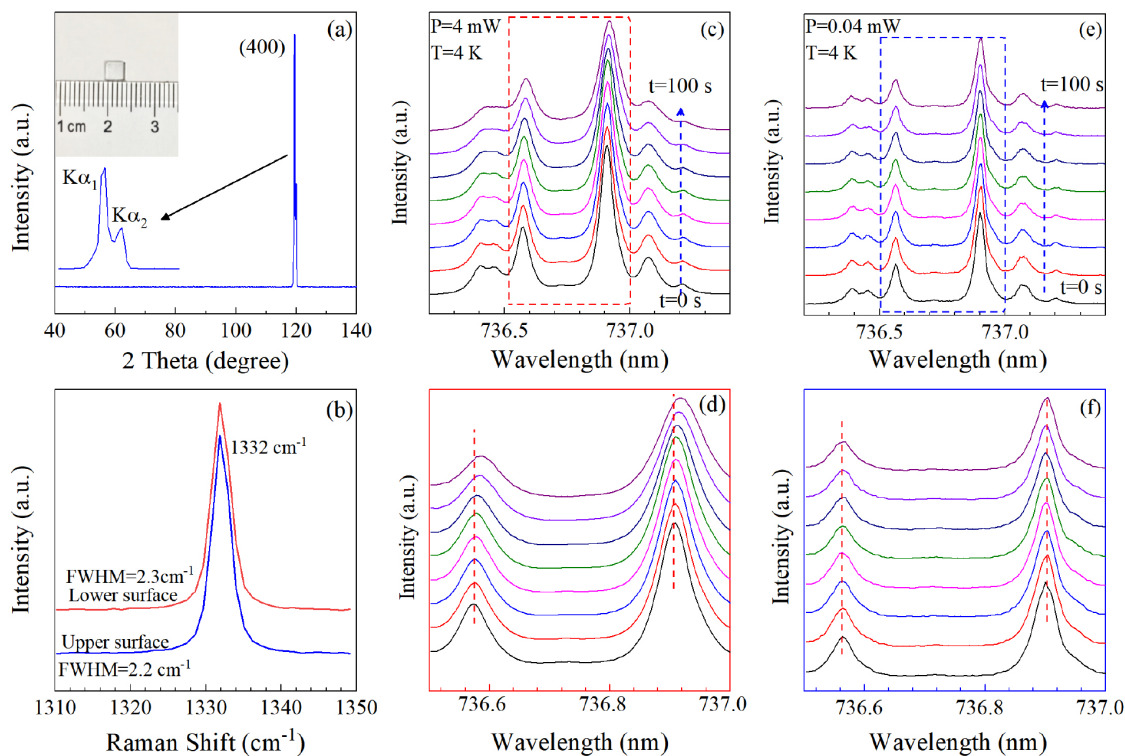


FIG. 1. The basic characterization of the CVD diamond and the time evolution of the fine structure spectra of SiV^- centers in diamond at 4 K under different excitation powers. (a) X-ray diffraction (XRD) pattern; the inset shows the optical image. (b) Raman spectra at the lower and upper surface. The lower and upper surfaces of the sample correspond to the beginning and end stages of sample growth, respectively. (c) and (e) Excitation powers are 4 and 0.04 mW at the lower surface, respectively. The spot area is about $4 \mu\text{m}^2$. (d) and (f) are enlarged for clarity.

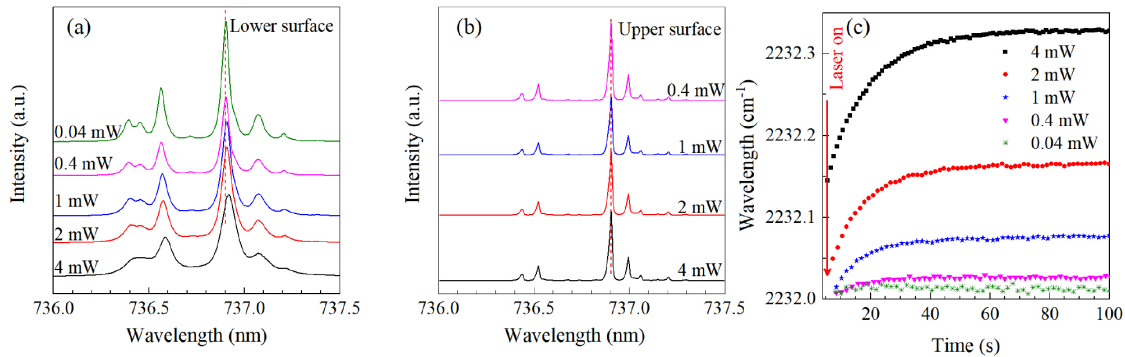


FIG. 2. The comparison of the fine structure spectra on the upper and lower surfaces. (a) and (b) Stable PL spectra of SiV^- centers in diamond under different excitation powers on the lower and upper surfaces, respectively. (c) The redshift of the strongest peak of the fine structure spectrum in the lower surface with time. The vertical axis is expressed as a relative wavenumber (cm^{-1}) with an excitation wavelength of 632.8 nm.

display the evolution of ZPL of the SiV^- ensemble under different excitation power. We note that the evolution of the fine structure spectra under 4 mW excitation has a significant redshift and broadening. Simultaneously, the PL intensity decreases. Under lower excitation power (0.04 mW), fluorescence spectra hardly change over time. Therefore, we infer that there is a laser heating effect in the high-power excitation process, which leads to a significant change in the fine structure spectra.

The heating effect seems to go against the perception that diamonds possess high thermal conductivity. Then, we made detailed measurements on the sample. Figures 2(a) and 2(b) show the fine structure spectra of SiV^- centers on the lower and upper surfaces at 4 K under different excitation power, respectively. Since the spectra evolve over time, the spectra shown here in the lower surface are the result after the final thermal stabilization. The fine structure spectra on the upper surface have no dependence on the power, while the spectra on the lower surface show a significant power dependence. In addition, the fine structure spectra in the upper and lower surfaces are significantly different and the linewidth of spectra in the lower surface is much wider than that in the upper surface. A crucial prerequisite to observe the SiV^- fine structure is a low strain crystal environment and defect concentration.^{25,26} When the strain is large or the defect concentration is relatively high, the fine structure widens and disappears. Therefore, the laser heating effect in the lower surface may be related to the residual stress and defect concentration.²³ The evolution of the fine structure spectra under different excitation powers was measured. Figure 2(c) shows the evolution of the peak position of the strongest peak over time. The peak position undergoes a significant redshift when the exciting power is greater than 0.04 mW. Under different excitation powers, the evolution time of the spectra is almost in the order of tens of seconds, which means that the thermal diffusion process is very slow.

In semiconductors, the heating of the lattice strongly influences the luminescence spectra. This is manifested in two ways in the PL spectra. First, the spectral distribution of PL intensity changes due to the increase in kinetic energy of photo-excited carriers.²⁷ Second, the peak position of photoluminescence shows an appreciable shift with temperature, which results from the variation in the energy of electronic states produced by anharmonic interaction of electrons and phonons.²⁸ The temperature dependence of the energy gap of

semiconductors is usually described by a semiempirical relation known as Varshni's equation.²⁹ In Fig. 3(a), the intrinsic temperature dependence of the SiV^- centers was measured under lower excitation power. We found the evolution of spectra with temperature is similar to that with time in Fig. 1(c). Figure 3(b) shows the peak shift (blue) of the strongest peak under different excitation powers and the intrinsic peak shift (red) with temperature under low-power excitation. The stable peak position under 4 mW excitation is almost consistent with the intrinsic peak position at 40 K; thus, the temperature at the center of the laser spot under 4 mW excitation is about 40 K, and the laser spot

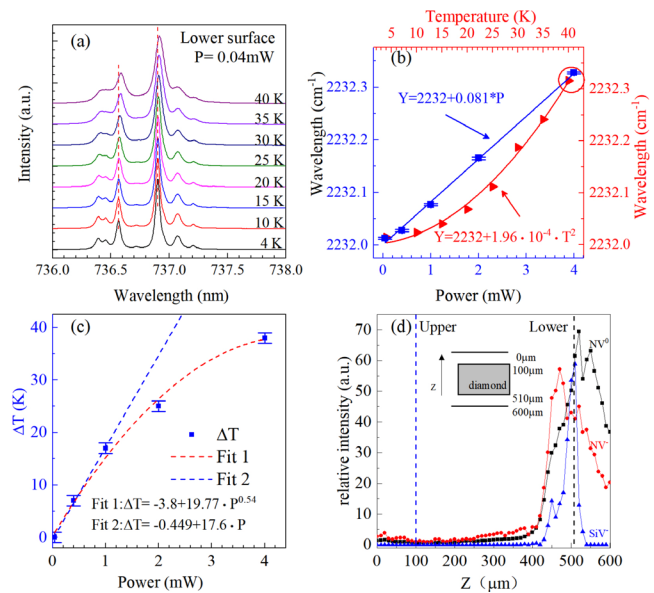


FIG. 3. (a) The intrinsic temperature-dependent PL spectra of SiV^- in the lower surface under 0.04 mW excitation. (b) The strongest peak position under different excitation power (blue) at 4 K, and temperature dependence of the peak position of the strongest peak under 0.04 mW excitation (red). (c) Temperature changes at the center of the laser spot under different excitation power. (d) Variation of defect concentration along the growth direction of the sample normalized by Raman peak at 1332 cm^{-1} .

center does have a noticeable temperature rise. According to the work of Bergman *et al.*,³⁰ the PL redshift is attributed to laser heating and heat-trapping. When the laser beam is focused on the surface of diamond, a part of the optical energy is absorbed by defects, causing transition processes. Only the energy in the nonradiative transition process is transformed into heat energy. According to the work of Yang *et al.*,³¹ under an excitation power of P , the power density of heat P_h can be expressed as

$$P_h = L(1 - \eta)FP. \quad (1)$$

Here, η is the total luminescence quantum yield, F is the fraction of incident light absorbed by defects, and L is a proportionality constant. When the laser power is steady, there is a relation between the power density of heat (P_h) and temperature at the heating area (T),

$$P_h \approx \kappa(T - T_0), \quad (2)$$

where κ is the coefficient, which is directly proportional to the thermal conductivity, and T_0 is the sample holder temperature. Thus, it has

$$L(1 - \eta)FP \approx \kappa(T - T_0) \Rightarrow T \approx \mu P + T_0, \quad (3)$$

where μ is a coefficient, and $\mu = L(1 - \eta)F/\kappa$. Under the same laser power, a larger μ leads to a stronger local heating effect. In Fig. 3(c), we found the local heating effect does not increase linearly with excitation power. Under low-power excitation, temperature changes exhibit a linear dependence on power (fit 2: $\Delta T = -0.449 + 17.6 \cdot P$). As the power increases, it begins to show a deviation from a linear dependency relationship. We can fit the data with a sublinear function (fit 1: $\Delta T = -3.8 + 19.77 \cdot P^{0.54}$) very well. The main reason is that: with the high-power excitation, the thermal conductivity increases with temperature.⁶ At room temperature, the thermal conductivity of diamond is much higher than that at 4 K and the larger thermal conductivity leads to the smaller μ . To verify the theory is reasonable, we performed the same experiments at room temperature and did not observe the redshift and broadening whether on the upper or lower surface of diamond. Previously, the temperature dependence of the interband transition energies can be described by a Bose–Einstein-type expression.³² The reason for peak shift and the exact temperature dependence have been discussed in the literature.^{29,33} Lattice expansion and temperature-dependent electron lattice interaction led to a temperature-dependent bandgap in diamond. However, in Neu's work,³⁴ they discuss the temperature dependence of fine structure in more detail and make corrections to previous work. They found their measured data are consistent with a temperature dependence. Our measurement results and fitting are consistent with them, as presented in Fig. 3(b). Under the same conditions, local heating effects were only observed on the lower surface. In Eq. (3), μ determines the magnitude of the laser heating effect under the same excitation power, and it is determined by the absorption coefficient and thermal conductivity. The larger the absorption coefficient and the smaller the thermal conductivity, the larger μ will be. Therefore, the reason for the different phenomena observed on the upper and lower surfaces comes from the large difference in thermal conductivity. Figure 3(d) shows the distribution of defect concentration in the growth direction of the sample. The defect concentration is estimated by PL intensity. We found the defect concentration on the lower surface is significantly higher than that on the upper surface. The thermal conductivity of diamond depends strongly on impurity concentration and crystal lattice

imperfection.⁶ For example, nitrogen, which can present in a large concentration in diamonds, up to 0.25 reduces the thermal conductivity by several times.³⁵ High defect concentration absorbs more laser and turns into heat, and low thermal conductivity leads to greater temperature rise. Therefore, the root cause is the high defect concentration on the lower surface.

In order to have a more intuitive understanding of the laser heating process, we used a simplified model to simulate the thermal diffusion process shown in Fig. 4. The detailed simulation process is shown in Fig. S3 of the supplementary material. Since the measurement process cannot quantify the absorbed energy, the simulation process here is qualitatively judged. The spot area of the laser is much smaller than the sample size, so the two-dimensional axisymmetric structure is used to simplify the thermal diffusion process. Figure 4(a) shows the isotherm distribution of the cross section during the temperature rise. Temperature spreads around the center of the spot and quickly reaches thermal stability. Next, we simulated the effects of excitation power and thermal conductivity on the thermal diffusion process as shown in Figs. 4(b) and 4(c). Consistent with Eq. (3), regardless of the change in thermal conductivity, the steady temperature varies nearly linearly with the excitation power. Also, the equilibrium time of the thermal diffusion process does not change significantly under different excitation power, which is consistent with the experimental results. The thermal diffusion process was observed to be a relatively slow process during the experiment. The relationship between thermal conductivity and thermal equilibrium time is simulated. Figure 4(d) shows the evolution of temperature at the center of the laser spot with different excitation powers over time, which is calibrated by the temperature-dependent photoluminescence in Fig. 3(b). The equilibrium time of the thermal diffusion process is strongly dependent on the thermal conductivity of the sample. Here, assuming that the diamond on the upper surface is an ideal high-quality single-crystal diamond, and its thermal conductivity is set to 100 W/(m K). Through simulation, it can be found that there is almost no temperature change on the upper surface in Fig. 4(f). For the lower surface of the diamond, when the thermal conductivity is set to 1 W/(m K), the temperature evolution in the center of the spot is almost the same as the experiments in Fig. 4(e). Therefore, we confirm that the high defect concentration on the lower surface results in the thermal conductivity being greatly reduced to nearly two orders of magnitude.

By studying the fine structure spectrum of SiV⁻ centers in diamonds at low temperatures, we observed the dependence of the spectra on the excitation power. Under high-power excitation, the spectra show obvious redshift and broadening. By studying the temperature dependence of the spectra under low-power excitation, we confirm that it is related to laser heating effects at the center of the laser spot. Through theoretical analysis, the temperature rising in the center of the spot is determined by the low thermal conductivity of the diamond at low temperature. The large introduction of defects and the lattice imperfection in the initial growth greatly reduce the thermal conductivity of diamond on the lower surface. It is shown the fine structure spectrum of SiV⁻ centers could be a sensitive probe for temperature sensing at low temperatures due to extremely narrow linewidth. Through simulation, we estimate that high defect conductivity concentrations degrade thermal conductivity by nearly two orders of magnitude. Our work not only demonstrates the superiority of SiV⁻ centers in

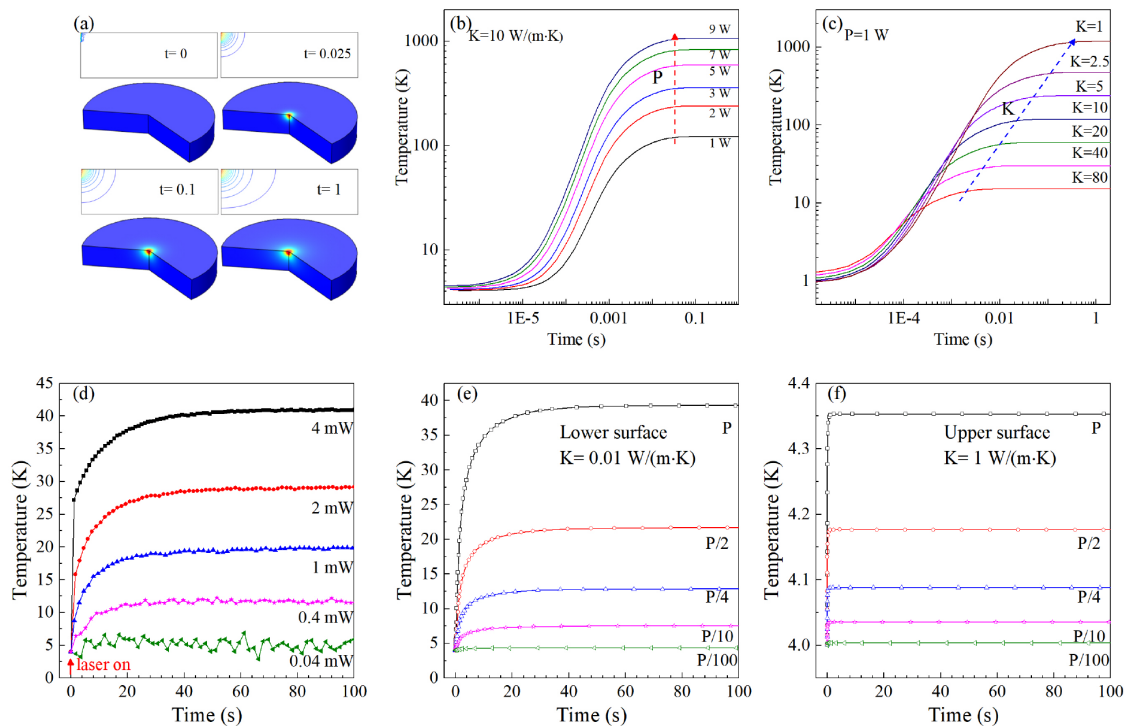


FIG. 4. The diffusion process simulation for laser heating. (a) Isotherm distribution in cross section and three-dimensional temperature distribution at different times, excitation power, and thermal conductivity is 1 W and 10 W/(m·K). (b) The evolution process of laser spot center temperature under different excitation powers when the thermal conductivity is 10 W/(m·K). (c) The evolution process of spot center temperature at different thermal conductivity when the excitation power is 1 W. The simulation of the relationship between thermal conductivity and equilibrium time. (d) The evolution of the temperature of the spot center under different excitation powers calibrated by the temperature-dependent photoluminescence spectra. (e) and (f) The temperature evolution process of the spot center under different thermal conductivity, respectively. Among them, 1 and 100 W/(m·K) are applicable to the lower surface and the upper surface of the diamond sample.

temperature sensing, but also provides an all optical non-contact temperature sensor, which helps to solve the problem of inaccurate measurement of thermal conductivity at cryogenic temperature.

See the supplementary material for additional details on the experimental methods and for additional data.

Authors acknowledge the funding support from the CAS Interdisciplinary Innovation Team, National Natural Science Foundation of China (Nos. 12074371, U1804155, and U1604263), and Research Equipment Development Project of Chinese Academy of Sciences (No. YJKYYQ20210001).

AUTHOR DECLARATIONS

Conflict of Interest

The authors have no conflicts to disclose.

Author Contributions

Yuanfei Gao: Investigation (lead); Writing – review & editing (lead). **Jia-Min Lai:** Investigation (supporting); Writing – original draft (supporting). **Zhen-Yao Li:** Writing – original draft (supporting). **Ping-Heng Tan:** Writing – review & editing (equal). **Chong-Xin Shan:** Writing – review & editing (equal). **Jun Zhang:** Writing – review & editing (lead).

DATA AVAILABILITY

The data that support the findings of this study are available within the article and its supplementary material.

REFERENCES

- G. A. Slack, “Nonmetallic crystals with high thermal conductivity,” *J. Phys. Chem. Solids* **34**, 321–335 (1973).
- Y. Zhang, F. Udrea, and H. Wang, “Multidimensional device architectures for efficient power electronics,” *Nat. Electron.* **5**, 723–734 (2022).
- J. W. Vandersande, “Boundary scattering in five natural type-II *a* diamonds,” *Phys. Rev. B* **13**, 4560–4567 (1976).
- L. Wei, P. K. Kuo, R. L. Thomas, T. R. Anthony, and W. F. Banholzer, “Thermal conductivity of isotopically modified single crystal diamond,” *Phys. Rev. Lett.* **70**, 3764–3767 (1993).
- D. G. Onn, A. Witek, Y. Z. Qiu, T. R. Anthony, and W. F. Banholzer, “Some aspects of the thermal conductivity of isotopically enriched diamond single crystals,” *Phys. Rev. Lett.* **68**, 2806–2809 (1992).
- A. V. Inyushkin, A. N. Taldenkov, V. G. Ralchenko, A. P. Bolshakov, A. V. Koliadin, and A. N. Katruska, “Thermal conductivity of high purity synthetic single crystal diamonds,” *Phys. Rev. B* **97**, 144305 (2018).
- G. Kucsko, P. C. Maurer, N. Y. Yao, M. Kubo, H. J. Noh, P. K. Lo, H. Park, and M. D. Lukin, “Nanometre-scale thermometry in a living cell,” *Nature* **500**, 54–58 (2013).
- J. M. Taylor, P. Cappellaro, L. Childress, L. Jiang, D. Budker, P. R. Hemmer, A. Yacoby, R. Walsworth, and M. D. Lukin, “High-sensitivity diamond magnetometer with nanoscale resolution,” *Nat. Phys.* **4**, 810–816 (2008).

- ⁹G. Balasubramanian, I. Y. Chan, R. Kolesov, M. Al-Hmoud, J. Tisler, C. Shin, C. Kim, A. Wojcik, P. R. Hemmer, A. Krueger, T. Hanke, A. Leitenstorfer, R. Bratschkis, F. Jelezko, and J. Wrachtrup, "Nanoscale imaging magnetometry with diamond spins under ambient conditions," *Nature* **455**, 648–651 (2008).
- ¹⁰T. T. Tran, B. Regan, E. A. Ekimov, Z. Mu, Y. Zhou, W.-b. Gao, P. Narang, A. S. Soltsev, M. Toth, I. Aharonovich, and C. Bradac, "Anti-stokes excitation of solid-state quantum emitters for nanoscale thermometry," *Sci. Adv.* **5**, eaav9180 (2019).
- ¹¹J.-F. Wang, L. Liu, X.-D. Liu, Q. Li, J.-M. Cui, D.-F. Zhou, J.-Y. Zhou, Y. Wei, H.-A. Xu, W. Xu, W.-X. Lin, J.-W. Yan, Z.-X. He, Z.-H. Liu, Z.-H. Hao, H.-O. Li, W. Liu, J.-S. Xu, E. Gregoryanz, C.-F. Li, and G.-C. Guo, "Magnetic detection under high pressures using designed silicon vacancy centres in silicon carbide," *Nat. Mater.* **22**, 489–494 (2023).
- ¹²V. N. Mochalin, O. Shenderova, D. Ho, and Y. Gogotsi, "The properties and applications of nanodiamonds," *Nat. Nanotechnol.* **7**, 11–23 (2012).
- ¹³D. Le Sage, K. Arai, D. R. Glenn, S. J. DeVience, L. M. Pham, L. Rahn-Lee, M. D. Lukin, A. Yacoby, A. Komeili, and R. L. Walsworth, "Optical magnetic imaging of living cells," *Nature* **496**, 486–489 (2013).
- ¹⁴S. Schmitt, T. Gefen, F. M. Stuerner, T. Uden, G. Wolff, C. Mueller, J. Scheuer, B. Naydenov, M. Markham, S. Pezzagna *et al.*, "Submillihertz magnetic spectroscopy performed with a nanoscale quantum sensor," *Science* **356**, 832–837 (2017).
- ¹⁵A. Sipahigil, R. E. Evans, D. D. Sukachev, M. J. Burek, J. Borregaard, M. K. Bhaskar, C. T. Nguyen, J. L. Pacheco, H. A. Atikian, C. Meuwly, R. M. Camacho, F. Jelezko, E. Bielejec, H. Park, M. Loncar, and M. D. Lukin, "An integrated diamond nanophotonics platform for quantum-optical networks," *Science* **354**, 847–850 (2016).
- ¹⁶S. Häußler, J. Benedikter, K. Bray, B. Regan, A. Dietrich, J. Twamley, I. Aharonovich, D. Hunger, and A. Kubanek, "Diamond photonics platform based on silicon vacancy centers in a single-crystal diamond membrane and a fiber cavity," *Phys. Rev. B* **99**, 165310 (2019).
- ¹⁷F. Dolde, H. Fedder, M. W. Doherty, T. Nöbauer, F. Rempp, G. Balasubramanian, T. Wolf, F. Reinhard, L. C. L. Hollenberg, F. Jelezko, and J. Wrachtrup, "Electric-field sensing using single diamond spins," *Nat. Phys.* **7**, 459–463 (2011).
- ¹⁸V. M. Acosta, E. Bauch, M. P. Ledbetter, A. Waxman, L. S. Bouchard, and D. Budker, "Temperature dependence of the nitrogen-vacancy magnetic resonance in diamond," *Phys. Rev. Lett.* **104**, 070801 (2010).
- ¹⁹S. Häußler, G. Thiering, A. Dietrich, N. Waasem, T. Teraji, J. Isoya, T. Iwasaki, M. Hatano, F. Jelezko, A. Gali, and A. Kubanek, "Photoluminescence excitation spectroscopy of SiV⁻ and GeV⁻ color center in diamond," *New J. Phys.* **19**, 063036 (2017).
- ²⁰J.-W. Fan, I. Cococar, J. Becker, I. V. Fedotov, M. H. A. Alkahtani, A. Alajlan, S. Blakley, M. Rezaee, A. Lyamkina, Y. N. Palyanov, Y. M. Borzdov, Y.-P. Yang, A. Zheltikov, P. Hemmer, and A. V. Akimov, "Germanium-vacancy color center in diamond as a temperature sensor," *ACS Photonics* **5**, 765–770 (2018).
- ²¹M. Fujiwara, G. Uchida, I. Ohki, M. Liu, A. Tsurui, T. Yoshikawa, M. Nishikawa, and N. Mizuochi, "All-optical nanoscale thermometry based on silicon-vacancy centers in detonation nanodiamonds," *Carbon* **198**, 57–62 (2022).
- ²²C. T. Nguyen, R. E. Evans, A. Sipahigil, M. K. Bhaskar, D. D. Sukachev, V. N. Agafonov, V. A. Davydov, L. F. Kulikova, F. Jelezko, and M. D. Lukin, "All-optical nanoscale thermometry with silicon-vacancy centers in diamond," *Appl. Phys. Lett.* **112**, 203102 (2018).
- ²³C. Hepp, T. Müller, V. Waselowski, J. Becker, B. Pingault, H. Sternschulte, D. Steinmüller-Nethl, A. Gali, J. Maze, M. Atatüre, and C. Becher, "Electronic structure of the silicon vacancy color center in diamond," *Phys. Rev. Lett.* **112**, 036405 (2014).
- ²⁴C.-N. Lin, Y.-J. Lu, X. Yang, Y.-Z. Tian, C.-J. Gao, J.-L. Sun, L. Dong, F. Zhong, W.-D. Hu, and C.-X. Shan, "Diamond-based all-carbon photodetectors for solar-blind imaging," *Adv. Opt. Mater.* **6**, 1800068 (2018).
- ²⁵H. Sternschulte, K. Thonke, J. Gerster, W. Limmer, R. Sauer, J. Spitzer, and P. C. Münzinger, "Uniaxial stress and Zeeman splitting of the 1.681 eV optical center in a homoepitaxial CVD diamond film," *Diamond Relat. Mater.* **4**, 1189–1192 (1995).
- ²⁶H. Sternschulte, K. Thonke, R. Sauer, P. C. Münzinger, and P. Michler, "1.681-eV luminescence center in chemical-vapor-deposited homoepitaxial diamond films," *Phys. Rev. B* **50**, 14554–14560 (1994).
- ²⁷C. S. Liu and J. F. Kauffman, "Photoluminescence and interfacial heat transfer in gallium arsenide," *Appl. Phys. Lett.* **75**, 1434–1436 (1999).
- ²⁸P. S. Dopal, H. D. Bist, S. K. Mehta, and R. K. Jain, "Laser heating and photoluminescence in GaAs and Al_xGa_{1-x}As," *Appl. Phys. Lett.* **65**, 2469–2471 (1994).
- ²⁹Y. P. Varshni, "Temperature dependence of the energy gap in semiconductors," *Physica* **34**, 149–154 (1967).
- ³⁰L. Bergman, X. B. Chen, J. L. Morrison, J. Huso, and A. P. Purdy, "Photoluminescence dynamics in ensembles of wide-band-gap nanocrystallites and powders," *J. Appl. Phys.* **96**, 675–682 (2004).
- ³¹Y. Yang, H. Yan, Z. Fu, B. Yang, L. Xia, Y. Xu, J. Zuo, and F. Li, "Photoluminescence investigation based on laser heating effect in ZnO-ordered nanostructures," *J. Phys. Chem. B* **110**, 846–852 (2006).
- ³²C. F. Li, Y. S. Huang, L. Malikova, and F. H. Pollak, "Temperature dependence of the energies and broadening parameters of the interband excitonic transitions in wurtzite GaN," *Phys. Rev. B* **55**, 9251–9254 (1997).
- ³³T. Feng and B. Schwartz, "Characteristics and origin of the 1.681 eV luminescence center in chemical-vapor-deposited diamond films," *J. Appl. Phys.* **73**, 1415–1425 (1993).
- ³⁴E. Neu, C. Hepp, M. Hauschild, S. Gsell, M. Fischer, H. Sternschulte, D. Steinmüller-Nethl, M. Schreck, and C. Becher, "Low-temperature investigations of single silicon vacancy colour centres in diamond," *New J. Phys.* **15**, 043005 (2013).
- ³⁵D. T. Morelli, T. A. Perry, and J. W. Farmer, "Phonon scattering in lightly neutron-irradiated diamond," *Phys. Rev. B* **47**, 131–139 (1993).